DOCUMENT 17

Physiological Chemistry and Physics

Volume 9, Number 1
1977

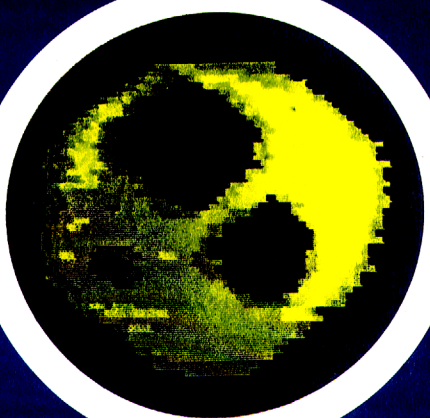

Sponsored by the International Society for Supramolecular Biology

Cross-sectional image by focused NMR (FONAR) of simulated chest. First FONAR image of live human chest appears on inside back cover, this issue. (Details on page 97 *et seq.*)

PLCHBA 9(1) 1-108 (1977)

Physiol. Chem. & Phys. 9 (1977)

NMR IN CANCER: XVI. FONAR IMAGE OF THE LIVE HUMAN BODY

R. DAMADIAN, M. GOLDSMITH, and L. MINKOFF
Department of Medicine and Program in Biophysics, State University of New York at Brooklyn, Downstate Medical Center, Brooklyn, New York 11203

• *The FONAR technique that achieved the first chemical image of the live human being is described. Color and black-and-white video images of a cross-section through the chest at the level of the eighth thoracic vertebra were generated. The imaging showed the heart and mediastinum in the midline between the left and right lungs with the heart encroaching on the left lung space as it does at this level. Also seen was the descending aorta just left and anterior to the vertebral body.*

Since the introduction in 1971 by Damadian of the nuclear resonance technique for detecting cancers, instrumentation has been under development for their visualization in live animals. The goal of these efforts by Damadian and co-workers has been a non-invasive means for visualizing not only tumors but also other biological structures in man. The method of Damadian has achieved this objective by focusing the NMR signal within the sample (FONAR).[1] This method was developed in 1972.[1] Subsequent methods have taken other approaches.[2-4]

In the NMR experiment, the irradiating ac field and the dc magnetic field applied across the sample must satisfy an exact ratio of frequency to field strength to obtain a signal from the sample. This ratio, the gyromagnetic ratio for the spinning nucleus, is a characteristic constant for each element and different for each magnetic nucleus. It is therefore possible by shaping the rf and dc fields within the sample to control the size of the resonating volume and thereby restrict, or focus, the signal-producing region within the sample to a small volume that can be examined independent of its surroundings.[3]

This resonating volume, or *FONAR resonance aperture* as we have designated it, can then be directed to any region within the interior of the sample for direct examination of the NMR chemistry of the locus, or it can be used to systematically scan through the sample to generate an image. The first tumor of a live animal was visualized by the FONAR method in 1976, utilizing a mouse with a tumor surgically implanted in the anterior thorax.[5] In the human, however, the largest structure subsequently possible to image by NMR has been the finger.[4] We wish now to report the achievement by FONAR of the first NMR images of the live human body, a cross-sectional visualization through the torso at the level of the eighth thoracic vertebra.

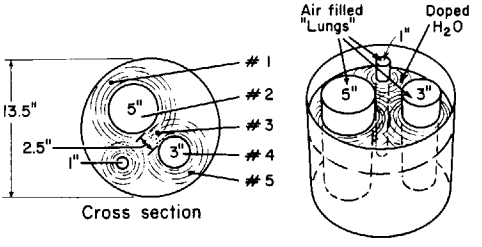

FIGURE 1. Schematic of the simulated (phantom) human chest used to obtain the FONAR image reproduced on the front cover of this issue of the journal. In the image, zero proton signal is color-coded blue while 3 shades of yellow represent the various signal intensities from doped H_2O. The phantom consisted of a cylindrical polypropylene tank (13.5 inches in diameter) filled with doped H_2O and containing 3 air-filled lucite cylinders with dimensions as indicated serving as "lungs." The numbered regions in the drawing correspond to the position of the FONAR spot for the NMR signals shown in Fig. 2. Note that the FONAR process easily detected the smallest structure in the phantom (1-inch "lung") with a 14-inch exploring coil (see front cover).

Experimental. To achieve this visualization we found it necessary to construct a superconducting magnet and cryogen designed to provide sufficient range in H_0 to maximize S/N and sufficient bore size to minimize inductive coupling of the human rf coil to the metallic mass of the magnet. A Helmholtz pair of superconductive magnets was constructed to optimize H_0 uniformity of the working field. The images presented in this paper, however, were achieved using only one of the pair, operating at 508 G. The details of construction of this magnet, and of the helium dewar, are given in the accompanying two papers of this series.

The rf pulses were delivered to a tape-wound 14-inch single-coil probe powered by a variable frequency Seimco model RD spectrometer operating at 2.18 MHz and delivering 10 W of power over 60 μsecs. 90° pulses were repeated with a period of 800 μseconds. The NMR images shown are stored video records of the maximum P-P amplitude of a constant 5-kc off-resonance beat pattern of the phase-detected proton signal. For the phantom chest, the off-resonance beat signal was visible without signal averaging because of the $NiCl_2$ doping of the H_2O. For the human chest, signal averaging was required. The proton images of the chest are therefore composites of

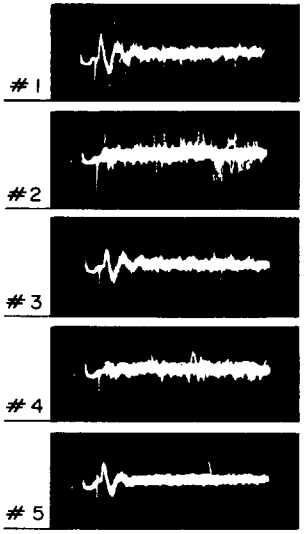

FIGURE 2. Off-resonance proton NMR signals (without signal averaging) from each of the numbered regions of the phantom shown in Fig. 1.

spin densities and spin-lattice relaxations, both contributing to variations in final signal amplitude and therefore to the various tissue intensities that make up the final image.

Phantom chest. For the first trial of the fully assembled FONAR apparatus, we utilized a simulated chest made up of a 13½-inch cylindrical container of $NiCl_2$-doped water with three air-filled methacrylate tubes of 5, 3, and 1 inches diameter respectively for "lungs." In these experiments the resonance aperture remained fixed along the H_0 axis and the sample was moved through it. Figure 1 gives a schematic of the phantom. The actual image is reproduced on the cover of this journal.

Figure 2 illustrates the signals observed, without averaging, as the phantom was moved along the x axis through regions of high proton density and low proton density. The experiment of Fig. 2 demonstrates prominent attributes of the FONAR method as compared to other methods in that (a) FONAR is direct, and (b) the FONAR signal is visible at each location of the scanning aperture. These capabilities allow the NMR behavior of each region of the anatomy to be visualized as the scan proceeds, rather than await a computer reconstruction of the data, as in the non-focusing methods, before information can be obtained. Furthermore, at the completion of the scan the resonance aperture can be directed back to the coordinates of a suspicious locus for more detailed examination.

Live human chest. On page 108 appears a schematic of a cross-section through the human chest at the level of the eighth thoracic vertebra. The FONAR image of the live human chest at that level is shown on the inside back cover of this journal. The scan visualized the heart and mediastinium, outlined a left lung cavity smaller than the right as it should be, detected a depression in spin density in the midline across the back that could correspond to the lowered proton density of the vertebral body, and encountered a high signal-producing region immediately anterior to the vertebral body and slightly to the left side of the thorax, which corresponds to the location of the descending aorta. We estimate the resolution of this image to be approximately ¼ inch.

Thus we completed the first chemical image of the human body, initiating a new era in medicine

[PLEASE TURN TO PAGE 108]

We wish to thank Bill and JoAnn Akers, Clarke and Eleanor Akers, James Stewart, and John Rich for the human charity that saw this project through to the finish. Were it not for their contributions, the work would not have been completed.

We thank Dr. Joel Stutman for the computer programs that produced the color video display. The imaging algorithm and related software he developed will be reported separately.

REFERENCES

1. R. Damadian, U.S. Patent 3,789,832, filed 17 March 1972.
2. W. S. Hinsbaw, "Image formation by nuclear magnetic resonance: The sensitive point method," *J. Applied Physics, 47*, 3709 (1976).
3. P. Mansfield and A. A. Maudsley, "Medical imaging by NMR," *Brit. J. Radiology, 50*, 188 (1977).
4. A. Kumar, D. Welti and R. R. Ernst, "NMR Fourier zeugmatography," *J. Magnetic Resonance, 18*, 69 (1975).
5. R. Damadian, L. Minkoff, M. Goldsmith, M. Stanford and J. Koutcher, "Field focusing nuclear magnetic resonance (FONAR): Visualization of a tumor in a live animal," *Science, 194*, 1430 (1976).

(Received July 6, 1977)

NMR IN CANCER: XVII. DEWAR FOR A 53-INCH SUPERCONDUCTING NMR MAGNET

L. MINKOFF, R. DAMADIAN, T. E. THOMAS, N. HU, M. GOLDSMITH, J. KOUTCHER, and M. STANFORD

Department of Medicine and Program in Biophysics, State University of New York at Brooklyn, Downstate Medical Center, Brooklyn, New York 11203

• *A giant nitrogen-jacketed liquid-helium metal dewar built in this laboratory is described for housing 53-inch superconducting magnet used in the human FONAR experiments. This dewar is 10 feet tall, 6 feet wide, 18 inches deep, and weighs 1½ tons. It consists of the main magnet hoop connected through a demountable gooseneck to a liquid helium reservoir tank.*

Of interest is the dewar built in our laboratory to contain the 53-inch superconducting NMR magnet described in the succeeding report of this series and utilized for human imaging by FONAR. The dewar provides 49 inches of working cavity and a maximum of flexibility for maintenance. Considered as a system, it (Fig. 1) may be separated into three sections: magnet hoop, storage can, and gooseneck.

1. Magnet hoop (detail, Fig. 1). This was built to maintain the magnet upright, z axis horizontal. The magnet is bolted into the liquid helium can, a doughnut-shaped stainless steel (type 304) tank we welded closed with a 300-A Airco TIG Heliwelder and thermally isolated by spacers (G-10 plastic, a glass-impregnated epoxy). The heat shield (6061-T6 aluminum) surrounding the helium section is conduction-cooled to 77°K by means of a second concentric doughnut containing liquid nitrogen. The heat shield was polished to a mirror finish to increase reflectivity and reduce helium loss due to radiation. Radiated heat transfer was further reduced by a wrapping of several layers of superinsulation (aluminized mylar, Metallized Products Division of King-Seeley Co., Winchester, Mass.) over the heat shield and also by a layer of aluminum tape (Emerson and Cuming, Canton, Mass.) wrapped on the liquid helium can. The nested doughnut sections, consisting of the liquid helium-magnet can surrounded by the nitrogen-cooled radiation shields, were encased in an outer vacuum jacket made of 6061-T6 ½-inch aluminum. We welded all the 6061 aluminum joints in the dewar with the 300-A Heliwelder. Seams and final dewar assembly were leak-checked with a Veeco model MS17-AM helium leak detector, and defective seams or porosities elsewhere in the metal were sealed with the welder.

Storage can (detail, Fig. 1). This consists of two liquid nitrogen reservoirs that bracket the liquid helium reservoir. The storage reservoirs for the cryogenic liquids are made of stainless steel (type 304) for strength and low heat conduction. The

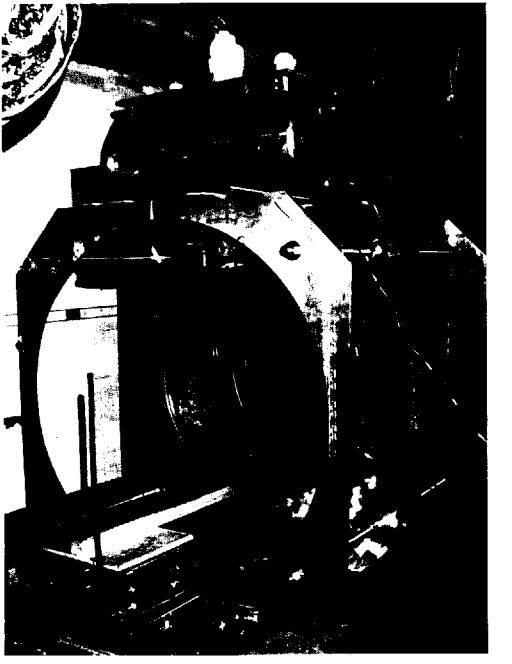

FIGURE 1. Photograph of the human "supercon" showing the main magnet hoop and parallel supports. The cylindrical helium storage can situated on top of the magnet joins it through a right-angle gooseneck (Fig. 2).

outer vacuum jacket of the storage can is made of aluminum (6061-T6). Joints between the steel storage cans and the aluminum outer jacket were made using bi-braze interfaces obtained from the Bi-Braze Corp. (Glen Head, N. Y.). Pressure manifolds, vents, and fill tubes were necessary to equalize nitrogen levels in the dual tank N_2 storage reservoir and for effective delivery of cryogenic liquid to the hoop.

Gooseneck (Fig. 2). A 2-inch stainless steel tube connecting the helium storage

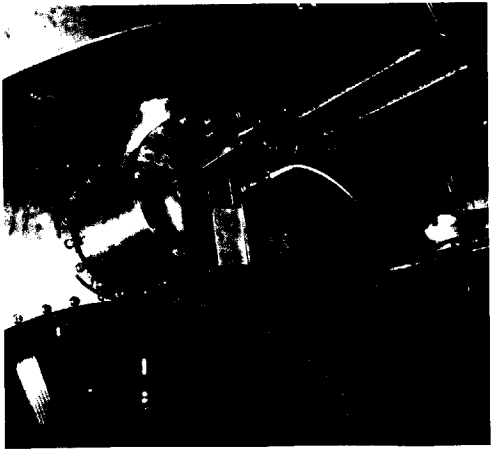

FIGURE 2. Dewar gooseneck with demountable header plate. Shown also are the hi-vac pumping port and Veeco Ion Pump mounted on the header.

can to the liquid helium reservoir of the hoop provides an excellent location for placement of the magnet "persistent" switches and superconductive joints. Repair of joints of persistent switches as needed can be accomplished through the gooseneck demountable header plate without dissembly of the main magnet dewar. The addition of a flexible metal bellows (Metal Bellows Corp., Sharon, Mass.) on the verticle arm of the gooseneck tube permitted easy removal of the switch plate from the helium tube.

Energizing the Magnet

The magnet is charged through a pair of 100-A demountable leads (American Magnetics Corp., Oak Ridge, Tenn.) that enter through the helium port in the top of the storage can and mate through a bayonet fitting to the main power leads mounted on a connector panel at the base of the storage can. A demountable Bendix connector, also coupling to the connector panel through the top helium port of the storage can, carries the heater leads for the superconductive switches, the level detector leads for storage can and hoop, and the voltage sensors for monitoring the magnet terminals during charging.

We wish to thank Dick Koch of Janis Research for the advice and counsel on dewar construction he gave without stint.

(Received July 6, 1977)

NMR IN CANCER: XVIII. A SUPERCONDUCTIVE NMR MAGNET FOR A HUMAN SAMPLE

M. GOLDSMITH, R. DAMADIAN, M. STANFORD, and M. LIPKOWITZ
Department of Medicine and Program in Biophysics, State University of New York at Brooklyn, Downstate Medical Center, Brooklyn, New York 11203

• *A 53-inch superconducting magnet built in our laboratory for human-size NMR is described. It was made from .026 inches superconducting wire laid on a 2.5-inch piece of channel bar that had been rolled into a 53-inch diameter circle and butt-welded at the ends.*

We give here a short account of our successful construction and testing of an NMR magnet with a 4-foot, 5-inch room temperature access. The magnet design is that of a Helmholtz pair. One of the magnet-dewar systems (i.e., half the complete system), now in operation for several months, was used in the human imaging reported in the initial paper of this series.

The magnet is wound on an aluminum former made from rolled channel bar. Its ends are butt-welded to close the circle. The channel dimensions are 2.5 by 1.25 inches. The windings were laid down using a winding machine we designed and built for the purpose. The machine is designed to feed wire automatically to the turning former by means of a motor-driven lead screw assembly and a motor-driven wire tension control. The time required to wind each magnet was approximately two weeks.

Each magnet contains a sweep coil and a Z-gradient coil in addition to the main magnet windings. The sweep and Z-gradient coils consist of two layers each of formvar-coated copper-clad niobium-titanium superconducting wire with a 12-mil diameter core and a total diameter of 0.026 inches. There are 76 turns to each layer. The main magnet consists of 5 layers of the same wire (76 turns per layer) and 47 layers (91 turns per layer) of formvar-coated copper-clad niobium-titanium wire with a core diameter of 10 mil and a total diameter of 22 mil. Each layer is insulated by two wraps of 0.5 mil mylar ribbon, and the windings are separated from the walls of the former by spacers 250 mil wide and machined from G-10 plastic. The outer layer of windings is secured in place by 0.5 mil hastaloid ribbon.

One of the novel features of this magnet is a plate capable of being removed from the dewar while the magnet remains fixed in place. Access to the plate is provided through a demountable header plate in a gooseneck joining the main magnet dewar to the helium reservoir tank (see Fig. 2 in preceding report). Superconductive joints,

TABLE I. Characteristics of the Human Magnet (each half)

Magnet bore diameter	53 inches
Inductance	61.8 henrys
Stored energy in the magnetic field (at 4 MHz)	2.97×10^7 joules
Stability (at 2.18 MHz)	7 parts in 10^9 over one hour
Magnet weight (without dewar)	120 pounds
Maximum field (theory)	5000 gauss
Maximum field (so far tested)	1000 gauss

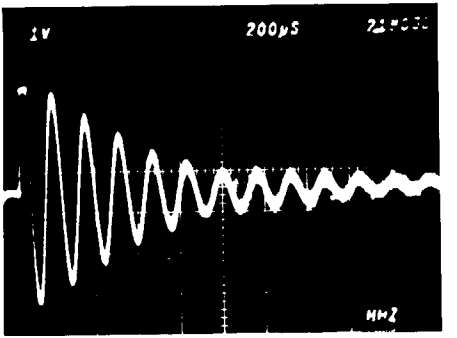

FIGURE 1. Off-resonance proton signal in the operating magnet half. This signal was obtained from a 1-inch sample of doped water in a single-probe saddle coil formed by a pair of cylindrical Helmholtz coils.

persistent switches, etc., are thereby all made accessible for repair without dissembly of the dewar. This plate contains all of the superconducting joints as well as the superconducting switches necessary to place the magnet into a "persistent" mode of operation. In addition, the plate houses all electrical connections necessary for operation of the main magnet and the other coils. Also incorporated, and essential to the operation of a magnet of high inductance, are protective devices against a sudden dumping of stored energy as well as high-resistance but low-power consumption (less than 300 mW) superconducting switches.

Although the magnet is theoretically capable of attaining a field of approximately

5000 G according to our computer calculations of the field mesh, our tests generally have been conducted with the magnet in persistent operation at either 500 or 1000 G. A preliminary estimate by NMR of the magnet's drift rate indicates that it is better than 7 parts in 10^7 over a one-hour period. In fact, to date there has been no NMR-detectable drift. Table I presents a short compilation of the properties of each magnet comprising the Helmholtz pair. Figure 1 shows a hydrogen off-resonance beat pattern obtained in the operating magnet half at 2.18 MHz using a 1-inch diameter single coil probe formed from a pair of cylindrical Helmholtz coils.

(Received July 6, 1977)

COLOR ILLUSTRATION ▼

A FONAR cross-section of the live human chest at the level of the 8th thoracic vertebra is reproduced on the back cover below. Proton signal intensity is color-coded, with dark blue assigned to zero signal amplitude and signals of increasing amplitude proceeding down the color look-up table (lower right inset) toward the yellow and white intensities. Top of image is anterior boundary of chest wall. Left area is left side of chest. Proceeding from anterior to posterior along midline, the principal structure is the heart seen encroaching on the left lung field (blue cavity). Left lung field is diminished in size relative to right lung (blue cavity to right of midline), as it should be (see schematic on this page of the human chest at the thoracic level of the FONAR image). More posteriorly and slightly left of midline is a red circular structure corresponding to the descending aorta.

In the body wall, beginning at the sternum (anterior midline) and proceeding around the ellipse, alternation of high intensity (yellow) with intermediate intensity (red) could correspond to alternation of intercostal muscles (high intensity) with rib (low intensity) as shown in the schematic.

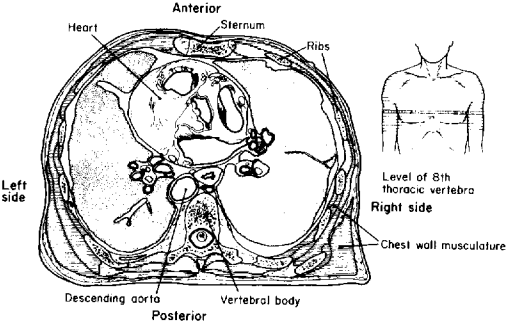

Human Chest (Cross Section)

[CONTINUED FROM PAGE 100]

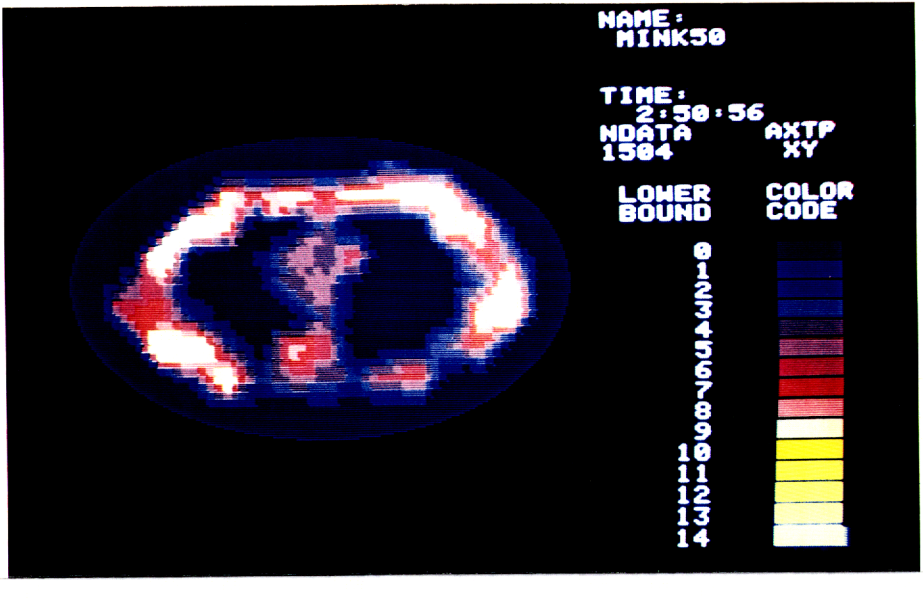
NAME:
MINK50
TIME:
2:30:56
NDATA
1504
AXTP
XY
LOWER BOUND
COLOR CODE
0
1
2
3
4
5
6
7
8
9
10
11
12
13
14

Volume 9 Number 1 1977
PHYSIOLOGICAL CHEMISTRY and PHYSICS

CONTENTS

Full Papers

C. TORDA. A Glycoprotein Fraction "Modulator" of Norepinephrine Effects *In Vivo* 3

J. N. UDALL, L. A. ALVAREZ, D. C. CHANG, H. SORIANO, B. L. NICHOLS, C. F. HAZLEWOOD. Effects of Cholera Enterotoxin on Intestinal Tissue Water as Measured by Nuclear Magnetic Resonance (NMR) Spectroscopy: II . . . 13

G. TORELLI, F. CELENTANO, G. CORTILI, E. D'ANGELO, A. CAZZANIGA, E. P. RADFORD. Hemoglobin-Oxygen Equilibrium at Different Hemoglobin and 2,3-Diphosphoglycerate Concentrations 21

J. C. RUSSELL and M. M. CHAMBERS. Effect of Histamine upon the Dynamics of Carbon Dioxide 39

C. W. GARNER and F. J. BEHAL. Fluorescence of Human Liver Alanine Aminopeptidase 47

D. D. FELLER, E. D. NEVILLE, S. ELLIS. *In Vivo* Response of Ornithine Decarboxylase Activity to Growth Hormone as Demonstrated by Oxidation of L-Ornithine-1-^{14}C in Hypophysectomized Rats 55

R. STROM, C. CRIFÒ, S. MARÌ, G. FEDERICI, I. MAVELLI, A. F. AGRO. Protoporphyrin IX Sensitized Photohemolysis: Stoichiometry of the Reaction and Repair by Reduced Glutathione 63

D. LITWINSKA and L. SZADURSKI-SZADUJKIS. Alpha Adrenergic Blocking Effect Exerted by Vitamin B_{15} 75

T. UBUKA, S. UMEMURA, Y. ISHIMOTO, M. SHIMOMURA. Transamination of L-Cysteine in Rat Mitochondria 91

Short Notes

A. R. TUNTURI and T. W. BARRETT. Tonotopic Pattern for Single Neurons in Dog Cortex, Using Elementary Signals 81

R. P. PATEL and M. R. OKUN. Hydroxylation of Tyrosine by Plant Peroxidase and Mushroom Tyrosinase, with and without Hydrazine, to Retard the Oxidation of Dopa 85

Supplement

R. DAMADIAN, M. GOLDSMITH, L. MINKOFF. NMR in Cancer: XVI. FONAR Image of the Live Human Body 97

L. MINKOFF, R. DAMADIAN, T. E. THOMAS, N. HU, M. GOLDSMITH. NMR in Cancer: XVII. Dewar for a 53-Inch Superconducting NMR Magnet . . . 101

M. GOLDSMITH, R. DAMADIAN, M. STANFORD, M. LIPKOWITZ. NMR in Cancer: XVIII. A Superconductive NMR Magnet for a Human Sample 105

PACIFIC PRESS, INC. *Printed in U.S.A.*